Phosphorylation by PKC and PKA regulate the kinase activity and downstream signaling of WNK4

Maria Castañeda-Bueno[a,b,c], Juan Pablo Arroyo[a,b], Junhui Zhang[a,b], Jeremy Puthumana[a,b], Orlando Yarborough III[a,b], Shigeru Shibata[a,b], Lorena Rojas-Vega[c,d], Gerardo Gamba[c,d], Jesse Rinehart[e], and Richard P. Lifton[a,b,f]

[a]Department of Genetics, Yale University School of Medicine, New Haven, CT 06510; [b]Howard Hughes Medical Institute, Yale University School of Medicine, New Haven, CT 06510; [c]Department of Nephrology and Mineral Metabolism, Instituto Nacional de Ciencias Médicas y Nutrición Salvador Zubirán, 14080 Mexico City, Mexico; [d]Molecular Physiology Unit, Instituto de Investigaciones Biomédicas, Universidad Nacional Autónoma de México, 14080 Mexico City, Mexico; [e]Department of Cellular and Molecular Physiology and Systems Biology Institute, Yale University School of Medicine, New Haven, CT 06510; and [f]Laboratory of Human Genetics and Genomics, The Rockefeller University, New York, NY 10065

Contributed by Richard P. Lifton, December 13, 2016 (sent for review September 20, 2016; reviewed by Thomas M. Coffman and David Pearce)

With-no-lysine kinase 4 (WNK4) regulates electrolyte homeostasis and blood pressure. WNK4 phosphorylates the kinases SPAK (Ste20-related proline alanine-rich kinase) and OSR1 (oxidative stress responsive kinase), which then phosphorylate and activate the renal Na-Cl cotransporter (NCC). WNK4 levels are regulated by binding to Kelch-like 3, targeting WNK4 for ubiquitylation and degradation. Phosphorylation of Kelch-like 3 by PKC or PKA downstream of AngII or vasopressin signaling, respectively, abrogates binding. We tested whether these pathways also affect WNK4 phosphorylation and activity. By tandem mass spectrometry and use of phosphosite-specific antibodies, we identified five WNK4 sites (S47, S64, S1169, S1180, S1196) that are phosphorylated downstream of AngII signaling in cultured cells and in vitro by PKC and PKA. Phosphorylation at S64 and S1196 promoted phosphorylation of the WNK4 kinase T-loop at S332, which is required for kinase activation, and increased phosphorylation of SPAK. Volume depletion induced phosphorylation of these sites in vivo, predominantly in the distal convoluted tubule. Thus, AngII, in addition to increasing WNK4 levels, also modulates WNK4 kinase activity via phosphorylation of sites outside the kinase domain.

renin-angiotensin-aldosterone system | NCC | hypertension | renal electrolyte transport | distal convoluted tubule

The distal portion of the mammalian nephron plays a key role in water, electrolyte, and blood pressure homeostasis. Mutations that alter normal renal Na-Cl homeostasis in this nephron segment modulate blood pressure and result in diverse electrolyte abnormalities (1). One such rare Mendelian trait is Pseudohypoaldosteronism type II (PHAII, OMIM 145260), which is characterized by hypertension, hyperkalemia, and metabolic acidosis; these features can be corrected by low doses of thiazide diuretics, inhibitors of the Na-Cl cotransporter of the distal convoluted tubule (NCC).

Genetic analysis of PHAII has revealed a previously unrecognized pathway that regulates blood pressure and electrolyte homeostasis in the distal nephron. Causative mutations have been found in four genes; two encode the serine–threonine kinases with-no-lysine 1 and 4 (WNK1 and WNK4) (2), and two encode Cullin 3 (CUL3) and Kelch-like 3 (KLHL3), components of an E3-RING ubiquitin ligase complex (3). At the time of the discovery of their causal relationship to this Mendelian disease, none of these proteins were known to play a role in electrolyte or blood pressure homeostasis. The biochemical mechanisms that link mutations to clinical phenoytpes are becoming understood. WNK4 is a Cl^--regulated kinase (4); when active, the kinase phosphorylates the kinases SPAK (Ste20-related proline alanine-rich kinase) and OSR1 (oxidative stress responsive kinase), which in turn phosphorylate and activate the thiazide-sensitive Na-Cl cotransporter of the renal distal convoluted tubule (DCT). The phenotype of WNK4 knockout (WNK4-KO) mice recapitulates Gitelman syndrome (OMIM 263800), the mirror image of PHAII, suggesting that in vivo WNK4 is mainly present in the active state and that it plays a central role in NCC regulation (5). In addition to this kinase-dependent regulation of the Na-Cl contransporter, WNK4 also regulates the activity of other mediators of distal renal electrolyte transport, for example, inhibiting the K^+ channel ROMK (6). It thus appears that increased WNK4 activity can explain the increased Na-Cl reabsorption and hypertension seen in PHAII; the inhibition of ROMK can explain the inability to excrete K^+, accounting for hyperkalemia (7). Inhibition of NCC activity can reverse both the hypertension and hyperkalemia seen with PHAII.

Nonetheless, the mechanisms that regulate the activity of WNK4 were obscure until the discovery that mutations in CUL3 and KLHL3 can also cause PHAII (3, 8). Subsequent work has shown that the kelch-like domain of KLHL3 specifically binds to WNK1 and WNK4, leading to their ubiquitylation and degradation (9, 10). Disease-causing dominant mutations in KLHL3 and CUL3 result in impaired binding and degradation of WNKs (9, 11, 12). Conversely, disease-causing mutations in WNK4 are predominantly missense mutations in a short acidic domain (2), which also prevent binding and ubiquitylation by the KLHL3–CUL3–RING complex; this acidic domain of WNK4 and WNK1 physically binds to KLHL3 (13).

Recent work has shown that the binding of WNK4 by KLHL3 is regulated by Angiotensin II (AngII) via protein kinase C (PKC). Activation of PKC by AngII results in phosphorylation of S433 in the kelch domain, preventing WNK4 binding (14). S433 is also targeted by PKA, presumably downstream of vasopressin

Significance

The kinase WNK4 (with-no-lysine kinase 4) is an important regulator of the Na-Cl cotransporter (NCC) in the renal distal convoluted tubule (DCT). Volume depletion induces angiotensin II, activating PKC, which prevents WNK4 degradation by phosphorylating the KLHL3/CUL3 ubiquitin ligase. We now show that PKC also directly phosphorylates WNK4 at multiple sites in cell culture. Phosphorylation of two of these sites, S64 and S1196, promotes increased WNK4 kinase activity by increasing autophosphorylation of the WNK4 T-loop at S332. Volume depletion also induces phosphorylation of WNK4-S64 in the DCT in vivo, promoting NCC activity. These findings provide insights into the mechanisms regulating activity of NCC and the promotion of renal Na-Cl reabsorption without concomitant K^+ secretion in volume depletion.

Author contributions: M.C.-B., S.S., G.G., J.R., and R.P.L. designed research; M.C.-B., J.P.A., J.Z., J.P., O.Y., L.R.-V., and J.R. performed research; M.C.-B., J.P.A., G.G., J.R., and R.P.L. analyzed data; and M.C.-B., J.P.A., G.G., J.R., and R.P.L. wrote the paper.

Reviewers: T.M.C., Duke–National University of Singapore Medical School Singapore; and D.P., University of California, San Francisco.

The authors declare no conflict of interest.

[1]To whom correspondence should be addressed. Email: rickl@rockefeller.edu.

This article contains supporting information online at www.pnas.org/lookup/suppl/doi:10.1073/pnas.1620315114/-/DCSupplemental.

(AVP) (15). The importance of this site is strongly supported by the observation that S433 is recurrently mutated in PHAII (3, 8). Thus, the level of WNK4 clearly plays a critical role in regulation of electrolyte homeostasis, with single amino acid substitutions that result in increased WNK4 levels, leading to hypertension and hyperkalemia in humans. This pathogenic mechanism is supported by studies of BAC-transgenic PHAII mice, which show that mutant WNK4 levels are elevated in vivo (9, 11).

These findings nonetheless leave open the question of whether elevated levels are all that is necessary for increased WNK4 activity. Specifically, we considered whether PKC and PKA, in addition to phosphorylating KLHL3, might also impart effects by phosphorylating WNK4. Consistent with this possibility, we noted that WNK4 contains multiple consensus sites for PKC and PKA. We report herein systematic identification of phosphorylation sites in WNK4 and demonstration of their effects on WNK4's biochemical function.

Results

WNK4 Phosphorylation Sites in HEK293 Cells. To examine steady-state Ser/Thr phosphorylation of WNK4, we expressed WNK4 tagged at the C terminus with the HA epitope in HEK293 cells and performed immunoprecipitation with anti-HA followed by mass spectrometry (MS) (16). Three mapping experiments were performed, capturing 56% of the WNK4 protein sequence. Eighteen phosphorylation sites were reproducibly identified (Fig. S1*A* and Table S1). Four of these sites were at RRXS motifs, which are commonly phosphorylated by PKC and PKA (S64, S1169, S1180, S1196); the peptide containing an additional RRXS motif, at Ser-47, was not observed in MS. The three most C-terminal RRXS sites are clustered and conserved across all vertebrates and lie close to functionally important domains (Fig. 1), whereas the two N-terminal sites are clustered and conserved in vertebrates, other than fish (Fig. 1*A*). Non-RRXS phosphorylation sites S1172 and S1176, which lie close to the C-terminal RRXS sites, and S332, which is the T-loop phosphorylation site required for activation of the kinase, are also highly conserved, whereas others are not at highly conserved positions in the protein (Table S1).

Activation of PKC and PKA Promotes Phosphorylation of WNK4–RRXS Sites. WNK4-HA–transfected COS-7 cells were treated acutely with the PKC inhibitor bisindolylmaleimide I (BIM), the PKC activator 12-O-tetradecanoylphorbol-13-acetate (TPA), or both. Changes in phosphorylation of WNK4–RRXS sites was examined by Western blotting using a well-established antibody with high specificity for RRXS^{P} (*Materials and Methods*). A clear WNK4–RRXS^{P} signal was detected in total cell extracts (Fig. 2*A*). TPA stimulation produced a significant increase in WNK4–RRXS phosphorylation (Fig. 2*A*) that was prevented in the presence of BIM. This finding strongly supports TPA-stimulated WNK4 phosphorylation because of activation of PKC rather than a different TPA-responsive kinase (17, 18). Because PKA also phosphorylates the RRXS motif (19), we probed the effect of pharmacologic inhibition and activation of PKA on WNK4–RRXS phosphorylation. Forskolin-induced PKA activation promoted WNK4–RRXS phosphorylation, which was prevented by coincubation with forskolin and PKA inhibitor, H89 (Fig. 2*B*).

To further demonstrate the direct effect of PKC and PKA on WNK4–RRXS phosphorylation, in vitro kinase reactions were performed. Purified PKCα (one of the most highly expressed diacylglycerol-dependent PKC isoforms in kidney epithelium) or PKA efficiently phosphorylated WNK4–RRXS sites, demonstrating that WNK4 is a substrate for in vitro phosphorylation by both kinases (Fig. S1 *B* and *C*).

Some of the RRXS sites in WNK4 have also been described as targets for serum glucocorticoid kinase 1 (SGK1)-mediated phosphorylation (20–22). However, TPA or forskolin-induced increases in WNK4–RRXS phosphorylation were not prevented by SGK1 inhibition with GSK65039 (23), suggesting that these effects were independent of SGK1 (Fig. S1 *D* and *E*).

PKC can be activated by AngII via downstream signaling via G_q and phospholipase C (24). COS-7 cells that express the AngII receptor show G_q-dependent activation of PKC in response to AngII (25). In these cells, we found that AngII promoted an increase in WNK4–RRXS phosphorylation within 10 min (Fig. 2*C*). This increase was prevented with BIM, consistent with AngII inducing PKC-dependent phosphorylation (Fig. 2*D*).

Phosphorylation of Individual Sites Probed with Phospho-Specific Antibodies. We developed phosphosite-specific antibodies for each of the five RRXS sites in WNK4 (*Materials and Methods*). Each of these was highly specific for phosphorylation at the specified site, as shown in each case by the loss of signal when the targeted serine residue was mutated to alanine (Fig. S2*A*).

Phosphorylation of each site was assessed in COS-7 and HEK293T cells following transfection with WNK4-HA and AT1 receptor and incubation with AngII, TPA (PKC activator), BIM (PKC inhibitor), forskolin (PKA activator), or H89 (PKA inhibitor). In both cell lines, treatment with AngII, TPA, and forskolin induced increased phosphorylation of all five sites (Fig. 3 *A* and *B* and Fig. S2 *B* and *C*). In addition, in vitro kinase assays performed with the purified PKCα and PKA produced phosphorylation of each of the five RRXS sites (Fig. 3*C*).

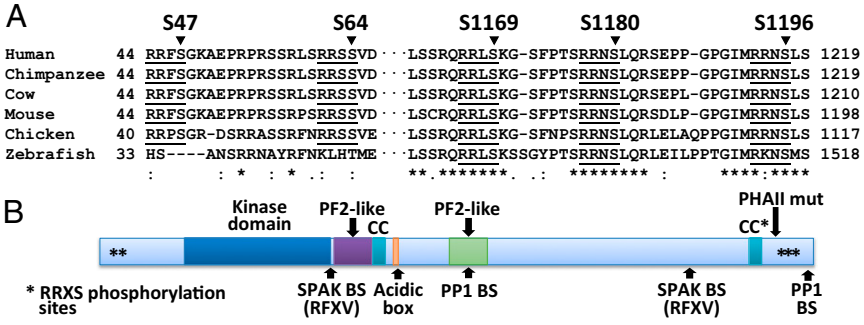

Fig. 1. Phosphorylation sites in WNK4 present within a RRXS sequence. (*A*) Alignment of amino acid sequences of WNK4 from different vertebrate species. The five RRXS motifs present in WNK4 and the phosphorylatable serine in each of them are indicated. Numbering corresponds to mouse WNK4. (*B*) Schematic representation of WNK4. Known domains and motifs are indicated. Location of the RRXS sites is shown with asterisks. CC, coiled-coil domain (2); CC*, coiled-coil domain that is implicated in WNK homo- and heterodimerization (39); PF2-like, domain similar to the PF2 domain present in SPAK/OSR1 (49); PP1-BS, protein phosphatase 1 binding site (50); SPAK-BS: SPAK binding site (49). PHAII-causing mutations found in WNK4 lie within the acidic box. Only one has been reported outside this region (R1185C; R1164C in mouse WNK4) (2) and its position is indicated. See also Tables S1 and S2.

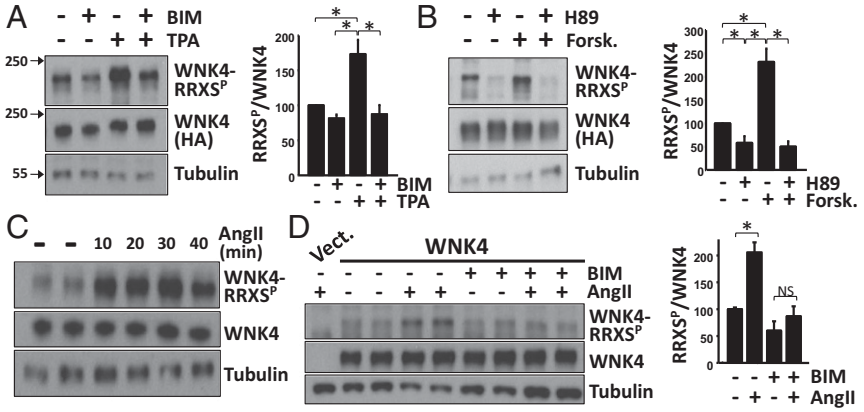

Fig. 2. Phosphorylation of WNK4–RRXS sites is triggered by AngII-PKC and PKA signaling. (*A*) WNK4-HA–transfected COS-7 cells were treated with the PKC inhibitor or activator, BIM (4 μM), or TPA (200 nM), respectively. Lysates were blotted with the RRXS^P antibody. (*B*) Same as in *A*, but cells were treated with the PKA inhibitor or activator, H89 (20 μM) or forskolin (30 μM), respectively. Bar graphs show the results of quantitation for *A* and *B* ($n = 5$). Data are means ± SEM; *$P < 0.05$. (*C*) COS-7 cells cotransfected with WNK4 and ATI were serum-depleted overnight and then stimulated with AngII (100 nM). AngII induced an increase in RRXS^P at all time points tested. (*D*) The indicated groups were preincubated with BIM for 15 min before stimulation with AngII (30 min). Blockade of PKC with BIM prevented the AngII-induced increase in WNK4–RRXS^P. Bar graphs summarize results of three experiments. Data are means ± SEM; *$P < 0.05$; NS, not significant. See also Fig. S1.

Functional Relevance of WNK4–RRXS Phosphorylation. We next evaluated the effect of RRXS phosphorylation on WNK4's kinase activity using a well-known target, SPAK, as a substrate. COS-7 cells were transfected with SPAK and WNK4 phosphorylation mutants. Cells were incubated with H89 or forskolin to alter WNK4 phosphorylation and SPAK phosphorylation (S373) was assessed (Fig. 4 *A*, *C*, and *D*, and Fig. S3). In the absence of WNK4, SPAK phosphorylation (pSPAK) levels were low and similar between H89- or forskolin-treated cells. However, in WNK4-transfected cells, pSPAK levels significantly increased despite the presence of H89, the PKA inhibitor, but were further augmented by forskolin (Fig. 4 *A* and *D*). This forskolin-induced increase in pSPAK was not observed in cells transfected with kinase inactive WNK4 (WNK4-KI; D318A) (26). Cotransfection of SPAK with a WNK4 (L319F mutant), which is not inhibitable by chloride (4, 27), promoted an even stronger increase in pSPAK that was again augmented by forskolin treatment (Fig. 4 *A*, *C*, and *D*). Mutation of all five serines in RRXS motifs to alanine (5A mutant) had no effect on WNK4 level, but drastically reduced the ability of WNK4 to phosphorylate SPAK. The 5A mutant showed pSPAK levels that were not significantly different from levels seen in the absence of WNK4, indicating a critical role of phosphorylation at these sites in modulation of WNK4's phosphorylation of SPAK. Furthermore, in the presence of this mutant, forskolin stimulation did not increase pSPAK, suggesting that phosphorylation of RRXS sites is necessary for this effect (Fig. 4 *A*, *C*, and *D*).

Similarly, AngII stimulation of HEK293T cells expressing WNK4 and SPAK also showed augmented SPAK phosphorylation that was abolished by the WNK4-5A mutations (Fig. 4 *B*, *E*, and *F*).

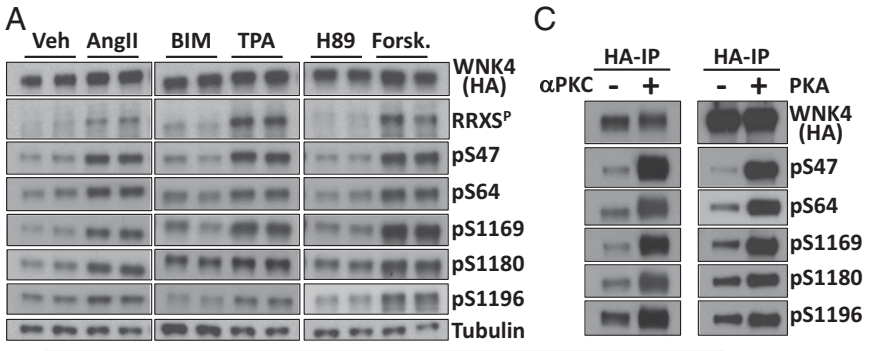

B

	Veh	AngII	P value	BIM	TPA	P value	H89	Forsk.	P value
RRXS^P	100	381	0.045	100	370	0.001	100	610	0.009
pS47	100	302	0.000	100	366	0.028	100	370	0.001
pS64	100	242	0.030	100	195	0.045	100	256	0.005
pS1169	100	333	0.011	100	207	0.003	100	342	0.013
pS1180	100	209	0.015	100	119	0.022	100	160	0.003
pS1196	100	200	0.042	100	135	0.008	100	220	0.027

Fig. 3. Characterization of WNK4 phosphorylation dynamics using phosphosite-specific antibodies. (*A*) COS-7 cells transfected with WNK4-HA and AT1 were stimulated with the indicated drugs for 30 min. Lysates were immunoblotted with the indicated antibodies. pS47, pS64, pS1169, pS1180, and pS1196 are WNK4 phosphosite-specific antibodies. (*B*) Results of quantitation of blots in *A* ($n \geq 4$, in at least three independent experiments). Band intensity values obtained with ImageJ were normalized, establishing vehicle, BIM, or H89 groups as 100%. (*C*) Immunopurified WNK4-HA was incubated with recombinant αPKC and PKA in the presence of all of the components necessary for kinase activity (30 min). Proteins were blotted with the indicated antibodies. See also Fig. S2.

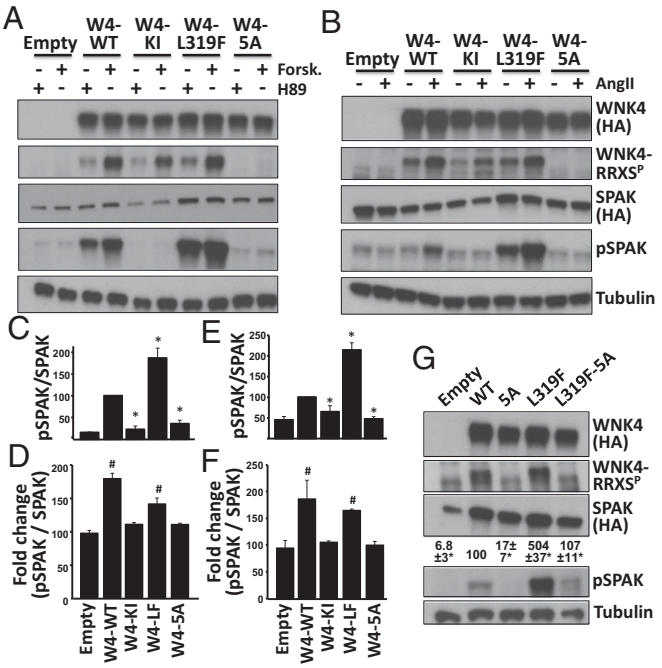

Fig. 4. Functional relevance of WNK4 phosphorylation in RRXS sites. (*A*) COS-7 cells were transfected with SPAK-HA and WNK4-HA or the indicated WNK4 mutants and stimulated with H89 (20 μM) or forskolin (30 μM). Lysates were blotted with the indicated antibodies. (*B*) HEK293T cells were transfected with SPAK-HA, ATI receptor and WNK4-HA, or the indicated mutants. After overnight serum depletion, cells were stimulated with vehicle or AngII (100 nM). Lysates were blotted with the indicated antibodies. KI, kinase inactive; 5A, mutant in which the Ser residues of the five RRXS motifs were substituted for Ala. (*C*) Quantitation of pSPAK/SPAK for H89-treated groups represented in *A*. (*D*) Fold-change in pSPAK/SPAK between H89 and forskolin groups. (*E*) Quantitation of pSPAK/SPAK for AngII-treated groups represented in *B*. (*F*) Fold-change in pSPAK/SPAK between vehicle and AngII groups. All data are means ± SEM; $n \geq 3$. $^*P < 0.05$ vs. WT; $^{\#}P < 0.05$ vs. Empty. Results of quantitation for RRXS^P and SPAK blots are shown in Fig. S3. (*G*) Cells were transfected with SPAK and different WNK4 mutants. Note that L319F-5A makes reference to a single clone that presents six mutations. SPAK phosphorylation was assessed. Results of quantitation are shown above pSPAK blot. All data are means ± SEM; $n = 3$. See also Figs. S3 and S4.

Interestingly, AngII did not induce increased pSPAK in cells cotransfected with WNK1 or WNK3 instead of WNK4 (Fig. S4 *A* and *B*), indicating that WNK4 is required for AngII-induced phosphorylation of SPAK (5).

To explore the hierarchy of regulatory mechanisms, we tested the activity of the chloride-insensitive mutant (W4-L319F) in the 5A mutant. This sextuple mutant showed markedly lower phosphorylation of SPAK than the W4-L319 mutant (Fig. 4*G*).

We next tested the importance of individual WNK4–RRXS phosphorylation sites on pSPAK and WNK4–RRXS^P levels in forskolin-stimulated COS-7 cells. We found that the S64A and S1196A mutations were the only ones that significantly reduced both total RRXS phosphorylation and SPAK phosphorylation (Fig. 5 *A* and *C* and Fig. S3*E*). When both mutations were present, the signal was virtually completely abolished. This observation, along with evidence that individual site mutations do not alter phosphorylation at other RRXS sites (Fig. S2*A*), suggests that S64 and S1196 are the main sites of WNK4 phosphorylation detected by the RRXS^P antibody and are the main sites required for phosphorylation of SPAK (Fig. 5 *A* and *C*). Similar results demonstrating the primacy of phosphorylation at S64 and S1196 in WNK4-mediated phosphorylation of SPAK were observed in HEK293T cells stimulated with AngII (Fig. 5 *B* and *D* and Fig. S3*F*).

Phosphorylation of S64 and S1196 Regulates Phosphorylation of the WNK4 T-Loop. Activation of WNK4 kinase is known to require autophosphorylation of S332 of the T-loop in the kinase catalytic domain (4, 28). We found that forskolin and AngII markedly increased T-loop phosphorylation, consistent with this being a primary mechanism by which forskolin and AngII increased downstream SPAK phosphorylation (Fig. 6). Moreover, we found that this increased phosphorylation at S332 was abolished following mutation of all RRXS sites; this effect was mediated by alanine substitution at S64 and S1196. In addition, we observed that AngII-induced S332 phosphorylation was dependent on PKC activation. In contrast, the alanine mutants showed no impairment of WNK4 binding to SPAK or protein phosphatase 1 (PP1) (Fig. S4 *C* and *D*). Thus, phosphorylation of these sites is implicated in the activation of WNK4 kinase activity rather than in WNK4's ability to bind to downstream targets or associated phosphatases.

Volume Depletion in Mice Promotes Phosphorylation of S64, S1169, S1180, and S1196. We used phosphosite-specific antibodies to test phosphorylation at specific sites in WNK4 in mouse kidney. Proteins from kidneys of WNK4-KO mice (5) were used to confirm the specificity of identified signals. We detected signal indicating phosphorylation at S64 and S1196 in Western blots of whole kidney protein extracts (Fig. S5*A*), and also at S1169 and S1180 in blots of renal extracts immunoprecipitated with anti-WNK4 (Fig. S6). We have not detected phosphorylation at S47 in either analysis.

We tested whether phosphorylation at these sites increases in response to AngII in the setting of volume depletion. As positive controls, we observed increased phosphorylation of T60 in NCC and increased levels of WNK4 (5, 14). We observed significantly increased phosphorylation of S64, S1169, S1180, and S1196 in the volume-depleted group (Fig. 7*A* and Fig. S6*A*). The ratio of pWNK4 to WNK4 was also significantly increased (Fig. 7*B* and Fig. S6*C*), indicating that WNK4 phosphorylation was stimulated and the increase was not simply the consequence of higher WNK4 levels. The increases in S64, S1169, S1180, and S1196 phosphorylation were not prevented by spironolactone (Fig. 7 *A* and *B* and Fig. S6 *B* and *D*), despite effective blockade of aldosterone signaling, as shown by blunting of the induction of SGK1 expression (Fig. S7*A*).

Volume Depletion Induces WNK4-S64 Phosphorylation Mainly in the DCT. To determine the renal cell types in which AngII increases phosphorylation of WNK4, we performed immunofluorescence microscopy using the anti-pS64 antibody, which gave a clear signal in volume-depleted wild-type mice that was eliminated in WNK4-KO mice (Fig. S5*B*). Staining was identified exclusively in nephron segments that also expressed NCC, localizing this phosphorylation to the DCT. As previously reported, NCC membrane abundance increased in the high AngII state (29). The staining patterns observed with the pS64-WNK4 and WNK4 antibodies were strikingly different between volume-depleted and volume-replete wild-type mice. In mice on a high salt diet, no pS64-WNK4 signal was detected in DCT cells (identified by NCC expression), whereas in volume-depleted mice, diffuse cytoplasmic staining with cytoplasmic puncta were clearly observed with anti-pS64 in all NCC-positive tubules (Fig. 7 *C*–*F*). Interestingly, this pattern of cytoplasmic puncta has been observed by others when staining with antibodies to SPAK, OSR1, and WNK4 (30, 31). We reproduced this pattern with antibodies to SPAK, OSR1, and pSPAK-S383 (Fig. S7 *B*–*G*). Costaining with WNK4-pS64 and SPAK, OSR1, or pSPAK antibodies revealed colocalization of these signals (Fig. S7 *H*–*J*).

S64 and S1196 Phosphorylation in PHAII Mice. We tested phosphorylation at S64 and S1196 in kidney samples from mice carrying

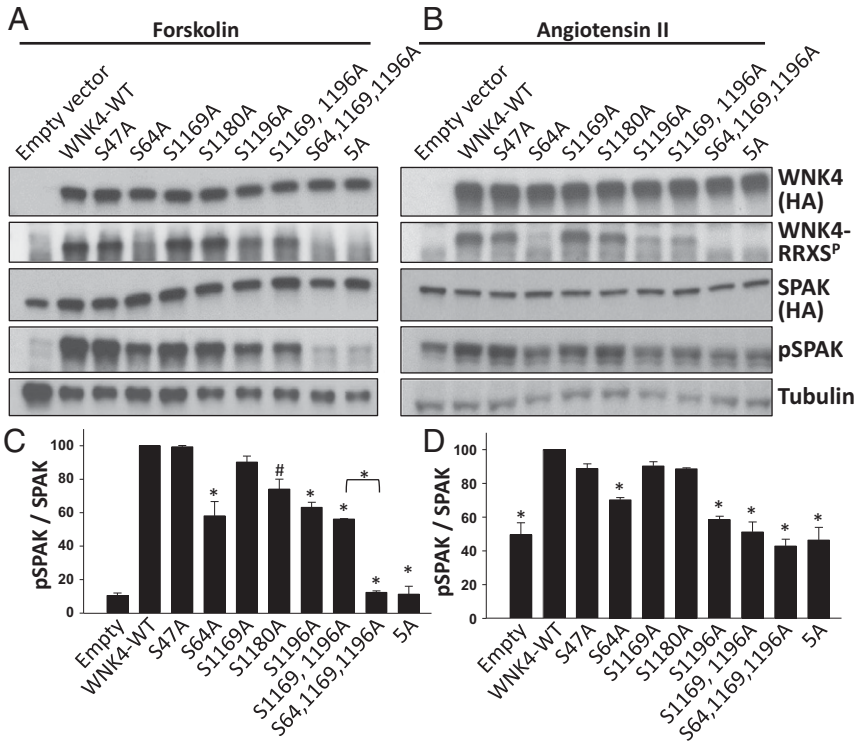

Fig. 5. Role of individual WNK4-RRXS^P sites in the regulation of WNK4-mediated SPAK phosphorylation. (*A*) COS-7 cells were transfected with SPAK-HA and WNK4-HA or the indicated WNK4 mutants. All cells were stimulated with forskolin (30 μM). Total cell extracts were blotted. (*B*) Same as in *A*, but instead HEK29T cells were used and cells were stimulated with AngII (100 nM). (*C* and *D*) Results of quantitation of pSPAK blots of *A* and *B*, respectively ($n = 3$). Band intensities were normalized establishing the WNK4-WT group as 100%. Data are means ± SEM. 5A, mutant in which the Ser residues of the five RRXS sites were substituted for Ala. $^*P < 0.01$; $^{\#}P < 0.05$. Quantitation for RRXS^P and SPAK blots is shown in Fig. S3.

a transgene with a WNK4–PHAII mutation (32). As expected, these mice had higher levels of WNK4 expression (Fig. 7 *G* and *H*). This result was accompanied by a higher level of S64 and S1196 phosphorylation. However, the fold-change in S64 phosphorylation and S1196 phosphorylation were, respectively, lower or similar to the fold-change observed for WNK4 total expression.

Discussion

The ability of increased renal salt reabsorption to cause hypertension is well established (1). AngII has been shown to promote renal Na^+ reabsorption in an aldosterone-independent manner (33–35), in part by increasing NCC activity (33) in a WNK4-dependent mechanism (5). We have previously shown that part of this mechanism is via increased levels of WNK4, because of AngII-PKC–mediated phosphorylation of KLHL3, which disrupts WNK4 binding and degradation (14). Here we describe an additional mechanism contributing to AngII's effect on WNK4. Upon AngII stimulation, PKC phosphorylates WNK4 sites, which in turn increase phosphorylation of the T-loop of WNK4, increasing kinase activity and phosphorylation of downstream targets. Prior work has shown that WNK4 regulates diverse electrolyte flux mediators by kinase-dependent and independent mechanisms. The ability to regulate kinase activity independently of WNK4 level permits differential regulation of downstream targets (7).

Of the two most critical PKC phosphorylation sites for kinase activation, serine 64 has not previously been reported, whereas S1196 has also been identified as a target of the aldosterone-induced kinase SGK1 (20–22). It seems clear that phosphorylation at this site is substantially attributable to direct phosphorylation by PKC/PKA because this site is directly phosphorylated by these enzymes in vitro, is regulated in cell culture by activators and inhibitors of PKC/PKA, and this site is phosphorylated in vivo by volume depletion despite inhibition of aldosterone signaling by spironolactone. We cannot exclude the possibility that PKC and PKA may phosphorylate additional sites in WNK4. For example, four phosphorylation sites identified by MS had variations of the PKC phosphorylation consensus sequence defined by basic amino acids at positions −3, −2, and +2, and in some cases, a hydrophobic amino acid at position +1 (36, 37) (Table S2).

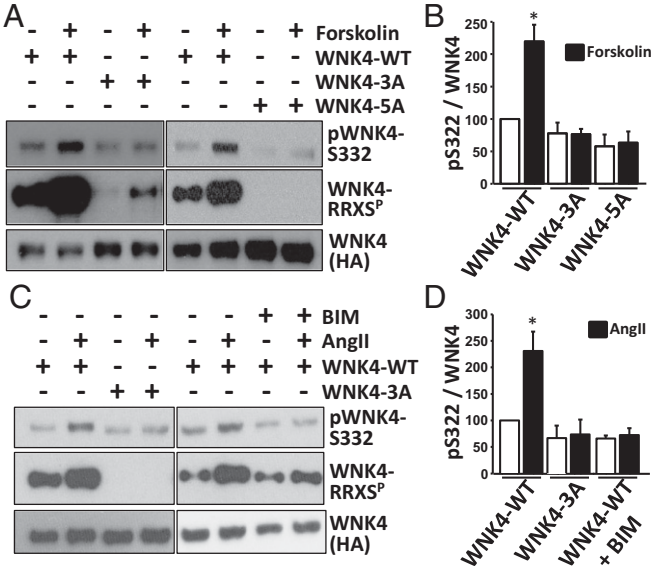

Fig. 6. WNK4-RRXS phosphorylation promotes WNK4 T-loop autophosphorylation. (*A*) WNK4 Ser-322 phosphorylation was assessed in immunoprecipitated WNK4 from HEK293 cells transfected with WNK4-WT, WNK4-3A (S64A, S1169A, S1196A) or WNK4-5A (S47A, S64A, S1169A, S1180A, S1196A) and stimulated with vehicle or forskolin for 30 min before lysis. (*B*) Results of quantitation. White bars, nonstimulated cells; Black bars, forskolin-stimulated cells. (*C*) Same as in *A*, but WNK4 Ser-322 phosphorylation was assessed in immunoprecipitated WNK4 from lysates of cells stimulated with vehicle or AngII for 30 min before lysis. The PKC inhibitor BIM was also added in the indicated groups. (*D*) Results of quantitation. White bars, nonstimulated cells; Black bars, AngII-stimulated cells. Data are means ± SEM; $^*P < 0.01$ vs. WT-nonstimulated (n = 3–6 in each group). See also Fig. S4 *C* and *D*.

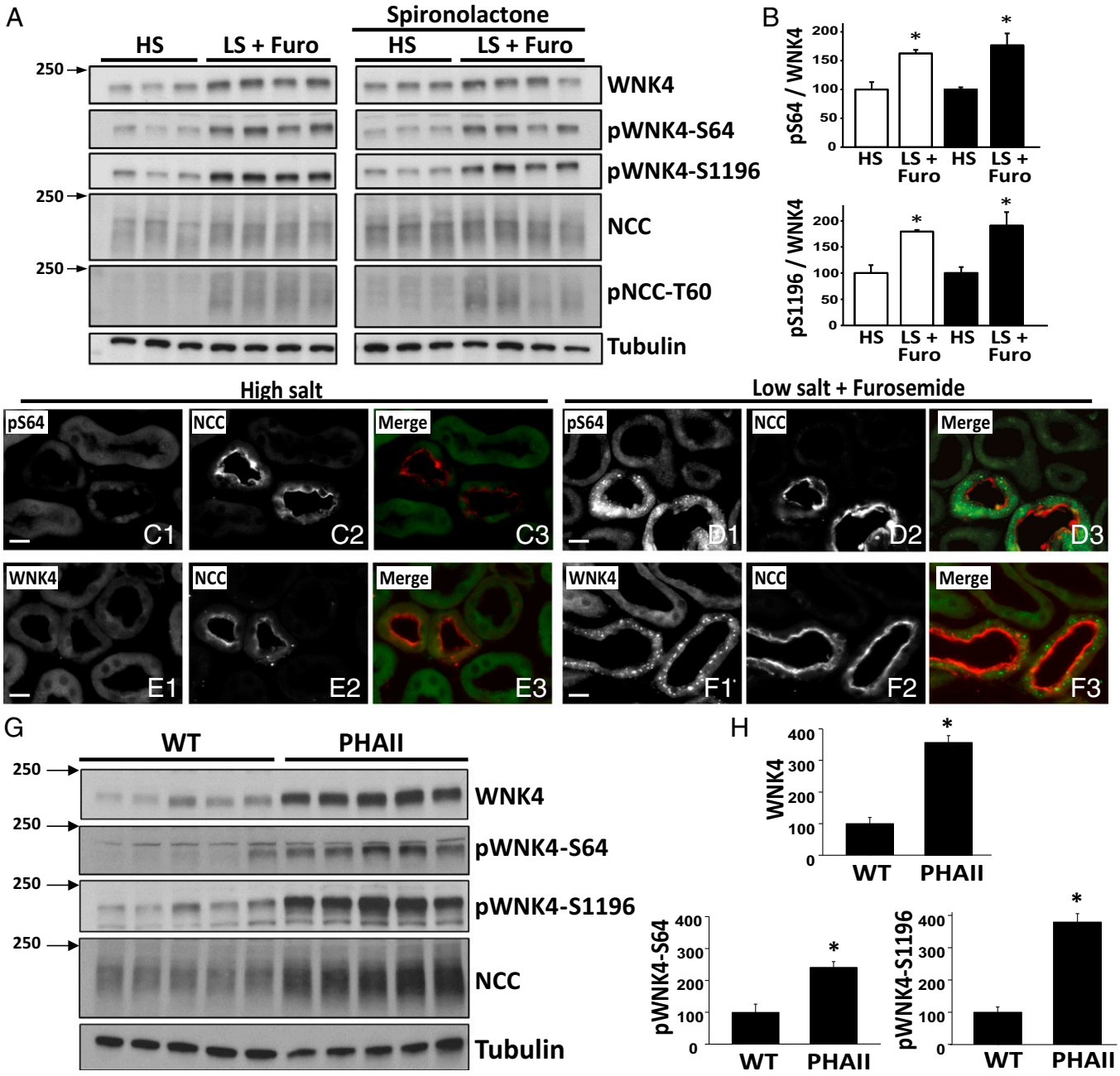

Fig. 7. In vivo phosphorylation of WNK4-S64 and S1196. (*A*) Mice were administered a low salt (LS) diet and given intraperitoneal furosemide for 3 d, or maintained on high salt (HS) diet and injected with vehicle. Treatments were replicated in two groups of mice, in which spironolactone was also administered. Kidney lysates were subjected to Western blot. Volume depletion promoted S64 and S1196 phosphorylation in mice. (*B*) Band intensities were quantified and the phosphorylated/total ratios were calculated. HS groups were established as 100%. White and black bars are groups without and with spironolactone treatment, respectively. Data are means ± SEM ($n = 6$ in each group). *$P < 0.05$. (*C–F*) Immunofluorescent staining of kidney sections from volume-replete and volume-depleted mice. Volume depletion-induced changes in signal intensity and staining pattern are observed in the DCTs of mice with the pS64-WNK4 and WNK4 antibodies. In the HS group, pS64 and WNK4 signals are virtually undetectable (*C* and *E*). (Scale bars, 10 μm.) (*G*) Kidney extracts from wild-type mice or PHAII mice carrying the WNK4–Q562E transgene (32) were blotted with the indicated antibodies. (*H*) Band intensities were quantified and results are presented relative to wild-type (100%). Data are expressed as means ± SEM; *$P < 0.05$. See also Figs. S5–S7.

Nevertheless, data show that elimination of S64 and S1196 is sufficient to prevent AngII-induced WNK4 activation.

It is interesting that the critical phosphorylation sites mediating the PKC/PKA-induced increase in WNK4 activity lie at the extreme amino and carboxyl-terminal ends of the protein. The N-terminal domain of WNK4 has previously been shown to have an inhibitory effect on WNK4 activity: when the N-terminal domain of WNK4 is substituted with the N-terminal domain of WNK3, the kinase becomes active in *Xenopus laevis* oocytes (38). Similarly, phosphorylation of S1196 has been shown to diminish WNK4's inhibitory effect on NCC in *X. laevis* oocytes, perhaps because of the attenuation of a dominant-negative effect (21). Our data suggest that phosphorylation of these sites via PKC/PKA relieves this inhibition via a mechanism that promotes phosphorylation of the T-loop of the kinase domain. This may occur via induction of a conformational change in WNK4, allowing access for intermolecular

T-loop phosphorylation (39), by reducing catalytic domain binding and inhibition by Cl^-, or by modulating the binding of an as yet unidentified protein that alters WNK4 activation.

In addition to PKC, we show that PKA also regulates WNK4. This finding is interesting because phosphorylation and activity of SPAK/OSR1-NCC is also increased by AVP (30, 40, 41). Binding of AVP to V2 receptors in renal epithelia leads to PKA activation; phosphorylation of WNK4 by PKA may be the next step mediating SPAK/OSR1-NCC activation.

PHAII is caused by increased activity of WNK1 and WNK4 (9, 11, 12). We propose that WNK4–RRXS phosphorylation is important for its activity; thus, we predict that WNK4–RRXS sites are phosphorylated in PHAII. Consistently, we observed that mice carrying a WNK4–PHAII mutation (32) have higher WNK4 expression and phosphorylation at S64 and S1196 (Fig. 7). The fold-change in pS1196, pS64, and WNK4 were similar; therefore, the higher phosphorylation observed may have been because of higher availability of substrate. Note that these sites are phosphorylated despite the low activity of the renin–angiotensin system. One possibility is that AVP-induced PKA activation may sustain RRXS phosphorylation. AVP levels have not been reported in PHAII patients or animals. However, AVP levels may be increased in states of increased salt reabsorption to maintain plasma isosmolarity, similar to the increased levels seen with high salt intake (42–44). Additionally, high plasma $[K^+]$ may also promote AVP secretion (45). It is also intriguing that in PHAII, WNK4 remains activated despite hyperkalemia, because high plasma K^+ would be expected to inhibit WNK activity by modulation of intracellular chloride (31).

Finally, these findings provide insight into the biochemical mechanism by which the kidney responds rapidly to reduce salt excretion in the setting of volume depletion (46). NCC activation by AngII occurs within minutes of the stimulus onset (29). AngII action, via WNK4 and SPAK, to activate NCC provides a response to volume depletion that is more rapid than the response via aldosterone, which requires time for adrenal induction of CYP11B2 mRNA and protein synthesis followed by aldosterone biosynthesis and its own induction of target genes in the kidney.

Materials and Methods

Cell Culture and Transient Transfection. COS-7 and HEK293T cells were used for transient expression of WNK4-HA, WNK4-FLAG, SPAK-HA, AT1R, WNK1-HA, and WNK3-HA. Cells were grown to 70–80% confluency and transfected with lipofectamine 2000 (Life Technologies). Forty-eight hours posttransfection, cells were lysed with a lysis buffer containing protease (Complete, Roche) and phosphatase inhibitors (Mixture 3, Sigma, P0044). Protein concentration was quantified by the BCA protein assay. Western blot assays and immunoprecipitation experiments were performed as described in *SI Materials and Methods*. Antibodies are also described. For treatment with BIM (Cell Signaling Technology #9841), TPA (Cell Signaling Technology #4174), H-89, Dihydrochloride (Cell Signaling Technology #9844), and forskolin (Cell Signaling Technology #3828), drugs were added to the culture media 30 min before lysis. The final concentration in the culture wells was 4 μM for BIM, 200 nM for TPA, 20 μM for H89, and 30 μM for forskolin. For acute treatment with AngII, cells were serum-depleted overnight and then incubated with 100 nM AngII for 30 min.

Mutations were introduced into the WNK4 clone by site directed mutagenesis using Pfu turbo DNA polymerase (Agilent) and confirmed by Sanger sequencing.

Phosphopeptide Enrichment and MS. The procedures followed were similar to those described previously (16). Briefly, HA-tagged WNK4 was immunoprecipitated from lysates of transiently transfected HEK293 cells and then resolved on SDS/PAGE. Protein bands were excised from the gel and digested in a trypsin solution (20 μg/mL, sequence grade; Promega). Extracted peptides were applied to pre-equilibrated TiO_2 TopTip microspin columns (Glygen). Eluate fractions were injected onto the HPLC column (Atlantis, 100 μm × 150 mm; Waters) directly interfaced to an electrospray ionization-quadrupole time-of-flight (ESI-QTOF) mass spectrometer (Waters/Micromass Q-Tof Ultima). Data were analyzed with Mascot 2.1 with improved phosphopeptide scoring. Identified phosphopeptides were confirmed by manual inspection of the spectra (for details see *SI Materials and Methods*).

Mouse Studies. Animal studies were approved by the Yale Institutional Animal Care and Use Committee (protocol no. 10018). Most studies were performed in wild-type C57BL/6 mice. WNK4-knockout and PHAII-transgenic mouse strains were also used (5, 32).

Volume-depletion model. Both the control and volume-depleted groups were kept on high salt diet [8% (wt/wt) NaCl] for ∼7 d before the beginning of treatment with furosemide. Half of the mice were then switched to low sodium diet (0.01–0.02% Na^+) and given intraperitoneal injections of furosemide (15 $mg{\cdot}kg^{-1}$, every 12 h for 3 d) (47). The control group was injected with saline and kept on high salt diet. Before being killed, mice were anesthetized with 100 $mg{\cdot}kg^{-1}$ ketamine plus 10 $mg{\cdot}kg^{-1}$ xylazine, the right renal artery was ligated, and the right kidney was collected and flash-frozen in liquid nitrogen. Mice were then perfused as described in *SI Materials and Methods* and the left kidney was harvested and treated as indicated for immunofluorescence (*SI Materials and Methods*).

Spironolactone treatment. The volume-depletion protocol was carried out as described in the previous section, but spironolactone was administered in both groups, control and furosemide-treated. Spironolactone treatment began 2 d before the first injection of furosemide and continued throughout experiment. Mice were injected every 12 h (intraperitoneally) with spironolactone (40 $mg{\cdot}kg^{-1}{\cdot}d^{-1}$) (48).

Statistical Analysis. For comparison between two groups, unpaired Student's *t* test (two tailed) was used. For comparison between multiple groups, ANOVA tests were performed, followed by Tukey post hoc tests. A difference between groups was considered significant when $P < 0.05$.

ACKNOWLEDGMENTS. We thank Carol Nelson-Williams for advice and helpful discussions; Dr. Jeremy Nichols (Parkinson's Institute and Clinical Center, Sunnyvale, CA) for kindly providing the PPIα clone; and Dr. David H. Ellison (Oregon Health & Science University, Portland, OR) for kindly providing the WNK4 antibody used for immunofluorescence studies. This work was supported by National Institutes of Health Grants P01DK17433 (to J.R. and R.P.L.), K01DK089006 (to J.R.), and R01DK51496 (to G.G.); Yale O'Brien Center Grant P30DK079310 (to P. Aronson and R.P.L.); and Conacyt Grants 165815 (to G.G.) and 257726 (to M.C.-B.).

1. Lifton RP, Gharavi AG, Geller DS (2001) Molecular mechanisms of human hypertension. *Cell* 104(4):545–556.
2. Wilson FH, et al. (2001) Human hypertension caused by mutations in WNK kinases. *Science* 293(5532):1107–1112.
3. Boyden LM, et al. (2012) Mutations in kelch-like 3 and cullin 3 cause hypertension and electrolyte abnormalities. *Nature* 482(7383):98–102.
4. Bazúa-Valenti S, et al. (2015) The Effect of WNK4 on the Na+-Cl- cotransporter is modulated by intracellular chloride. *J Am Soc Nephrol* 26(8):1781–1786.
5. Castañeda-Bueno M, et al. (2012) Activation of the renal Na+:Cl- cotransporter by angiotensin II is a WNK4-dependent process. *Proc Natl Acad Sci USA* 109(20):7929–7934.
6. Kahle KT, et al. (2003) WNK4 regulates the balance between renal NaCl reabsorption and K+ secretion. *Nat Genet* 35(4):372–376.
7. Hadchouel J, Ellison DH, Gamba G (2016) Regulation of renal electrolyte transport by WNK and SPAK-OSR1 kinases. *Annu Rev Physiol* 78(1):367–389.
8. Louis-Dit-Picard H, et al.; International Consortium for Blood Pressure (ICBP) (2012) KLHL3 mutations cause familial hyperkalemic hypertension by impairing ion transport in the distal nephron. *Nat Genet* 44(4):456–460, S1–S3.
9. Shibata S, Zhang J, Puthumana J, Stone KL, Lifton RP (2013) Kelch-like 3 and Cullin 3 regulate electrolyte homeostasis via ubiquitination and degradation of WNK4. *Proc Natl Acad Sci USA* 110(19):7838–7843.
10. Wakabayashi M, et al. (2013) Impaired KLHL3-mediated ubiquitination of WNK4 causes human hypertension. *Cell Reports* 3(3):858–868.
11. Susa K, et al. (2014) Impaired degradation of WNK1 and WNK4 kinases causes PHAII in mutant KLHL3 knock-in mice. *Hum Mol Genet* 23(19):5052–5060.
12. McCormick JA, et al. (2014) Hyperkalemic hypertension-associated cullin 3 promotes WNK signaling by degrading KLHL3. *J Clin Invest* 124(11):4723–4736.
13. Schumacher FR, Sorrell FJ, Alessi DR, Bullock AN, Kurz T (2014) Structural and biochemical characterization of the KLHL3-WNK kinase interaction important in blood pressure regulation. *Biochem J* 460(2):237–246.
14. Shibata S, et al. (2014) Angiotensin II signaling via protein kinase C phosphorylates Kelch-like 3, preventing WNK4 degradation. *Proc Natl Acad Sci USA* 111(43):15556–15561.
15. Yoshizaki Y, et al. (2015) Impaired degradation of WNK by Akt and PKA phosphorylation of KLHL3. *Biochem Biophys Res Commun* 467(2):229–234.
16. Rinehart J, et al. (2009) Sites of regulated phosphorylation that control K-Cl cotransporter activity. *Cell* 138(3):525–536.
17. Springett GM, Kawasaki H, Spriggs DR (2004) Non-kinase second-messenger signaling: New pathways with new promise. *BioEssays* 26(7):730–738.
18. Wilkinson SE, Parker PJ, Nixon JS (1993) Isoenzyme specificity of bisindolylmaleimides, selective inhibitors of protein kinase C. *Biochem J* 294(Pt 2):335–337.

19. Songyang Z, Cantley LC (1998) The use of peptide library for the determination of kinase peptide substrates. *Methods Mol Biol* 87:87–98.
20. Ring AM, et al. (2007) An SGK1 site in WNK4 regulates Na+ channel and K+ channel activity and has implications for aldosterone signaling and K+ homeostasis. *Proc Natl Acad Sci USA* 104(10):4025–4029.
21. Rozansky DJ, et al. (2009) Aldosterone mediates activation of the thiazide-sensitive Na-Cl cotransporter through an SGK1 and WNK4 signaling pathway. *J Clin Invest* 119(9):2601–2612.
22. Na T, Wu G, Zhang W, Dong WJ, Peng JB (2013) Disease-causing R1185C mutation of WNK4 disrupts a regulatory mechanism involving calmodulin binding and SGK1 phosphorylation sites. *Am J Physiol Renal Physiol* 304(1):F8–F18.
23. Sherk AB, et al. (2008) Development of a small-molecule serum- and glucocorticoid-regulated kinase-1 antagonist and its evaluation as a prostate cancer therapeutic. *Cancer Res* 68(18):7475–7483.
24. de Gasparo M, Catt KJ, Inagami T, Wright JW, Unger T (2000) International union of pharmacology. XXIII. The angiotensin II receptors. *Pharmacol Rev* 52(3):415–472.
25. Hansen JL, et al. (2009) Lack of evidence for AT1R/B2R heterodimerization in COS-7, HEK293, and NIH3T3 cells: how common is the AT1R/B2R heterodimer? *J Biol Chem* 284(3):1831–1839.
26. Wilson FH, et al. (2003) Molecular pathogenesis of inherited hypertension with hyperkalemia: The Na-Cl cotransporter is inhibited by wild-type but not mutant WNK4. *Proc Natl Acad Sci USA* 100(2):680–684.
27. Piala AT, et al. (2014) Chloride sensing by WNK1 involves inhibition of autophosphorylation. *Sci Signal* 7(324):ra41.
28. Zagórska A, et al. (2007) Regulation of activity and localization of the WNK1 protein kinase by hyperosmotic stress. *J Cell Biol* 176(1):89–100.
29. Sandberg MB, Riquier AD, Pihakaski-Maunsbach K, McDonough AA, Maunsbach AB (2007) ANG II provokes acute trafficking of distal tubule Na+-Cl(-) cotransporter to apical membrane. *Am J Physiol Renal Physiol* 293(3):F662–F669.
30. Saritas T, et al. (2013) SPAK differentially mediates vasopressin effects on sodium cotransporters. *J Am Soc Nephrol* 24(3):407–418.
31. Terker AS, et al. (2015) Potassium modulates electrolyte balance and blood pressure through effects on distal cell voltage and chloride. *Cell Metab* 21(1):39–50.
32. Lalioti MD, et al. (2006) Wnk4 controls blood pressure and potassium homeostasis via regulation of mass and activity of the distal convoluted tubule. *Nat Genet* 38(10): 1124–1132.
33. van der Lubbe N, et al. (2011) Angiotensin II induces phosphorylation of the thiazide-sensitive sodium chloride cotransporter independent of aldosterone. *Kidney Int* 79(1): 66–76.
34. Mamenko M, et al. (2013) Chronic angiotensin II infusion drives extensive aldosterone-independent epithelial Na+ channel activation. *Hypertension* 62(6):1111–1122.
35. Crowley SD, et al. (2011) Role of AT_1 receptor-mediated salt retention in angiotensin II-dependent hypertension. *Am J Physiol Renal Physiol* 301(5):F1124–F1130.
36. Pearson RB, Kemp BE (1991) Protein kinase phosphorylation site sequences and consensus specificity motifs: tabulations. *Methods Enzymol* 200:62–81.
37. Nishikawa K, Toker A, Johannes FJ, Songyang Z, Cantley LC (1997) Determination of the specific substrate sequence motifs of protein kinase C isozymes. *J Biol Chem* 272(2):952–960.
38. San-Cristobal P, Ponce-Coria J, Vázquez N, Bobadilla NA, Gamba G (2008) WNK3 and WNK4 amino-terminal domain defines their effect on the renal Na+-Cl- co-transporter. *Am J Physiol Renal Physiol* 295(4):F1199–F1206.
39. Thastrup JO, et al. (2012) SPAK/OSR1 regulate NKCC1 and WNK activity: Analysis of WNK isoform interactions and activation by T-loop trans-autophosphorylation. *Biochem J* 441(1):325–337.
40. Pedersen NB, Hofmeister MV, Rosenbaek LL, Nielsen J, Fenton RA (2010) Vasopressin induces phosphorylation of the thiazide-sensitive sodium chloride cotransporter in the distal convoluted tubule. *Kidney Int* 78(2):160–169.
41. Mutig K, et al. (2010) Short-term stimulation of the thiazide-sensitive Na+-Cl- co-transporter by vasopressin involves phosphorylation and membrane translocation. *Am J Physiol Renal Physiol* 298(3):F502–F509.
42. Cowley AW, Jr, Skelton MM, Merrill DC, Quillen EW, Jr, Switzer SJ (1983) Influence of daily sodium intake on vasopressin secretion and drinking in dogs. *Am J Physiol* 245(6):R860–R872.
43. Matsuguchi H, Schmid PG, Van Orden D, Mark AL (1981) Does vasopressin contribute to salt-induced hypertension in the Dahl strain? *Hypertension* 3(2):174–181.
44. Kjeldsen SE, et al. (1985) Dietary sodium intake increases vasopressin secretion in man. *J Clin Hypertens* 1(2):123–131.
45. Riphagen IJ, et al. (2016) Effects of potassium supplementation on markers of osmoregulation and volume regulation: Results of a fully controlled dietary intervention study. *J Hypertens* 34(2):215–220.
46. Rafiqi FH, et al. (2010) Role of the WNK-activated SPAK kinase in regulating blood pressure. *EMBO Mol Med* 2(2):63–75.
47. Lee CT, Chen HC, Lai LW, Yong KC, Lien YH (2007) Effects of furosemide on renal calcium handling. *Am J Physiol Renal Physiol* 293(4):F1231–F1237.
48. Castañeda-Bueno M, et al. (2014) Modulation of NCC activity by low and high K(+) intake: Insights into the signaling pathways involved. *Am J Physiol Renal Physiol* 306(12):F1507–F1519.
49. Gagnon KB, Delpire E (2012) Molecular physiology of SPAK and OSR1: Two Ste20-related protein kinases regulating ion transport. *Physiol Rev* 92(4):1577–1617.
50. Lin DH, et al. (2012) Protein phosphatase 1 modulates the inhibitory effect of With-no-Lysine kinase 4 on ROMK channels. *Am J Physiol Renal Physiol* 303(1):F110–F119.
51. Rinehart J, et al. (2011) WNK2 kinase is a novel regulator of essential neuronal cation-chloride cotransporters. *J Biol Chem* 286(34):30171–30180.
52. Richardson C, et al. (2008) Activation of the thiazide-sensitive Na+-Cl- cotransporter by the WNK-regulated kinases SPAK and OSR1. *J Cell Sci* 121(Pt 5):675–684.